Journal of Hydroscience and Hydraulic Engineering
Vol. 2, No. 2, November, 1984, pp.11-33.

LONGITUDINAL AND TRANSVERSE VARIATIONS OF THE DEPTH-AVERAGED FLOW FIELDS IN A MEANDERING CHANNEL

By

Nobuyuki Tamai

Professor, Department of Civil Engineering
University of Tokyo, Tokyo 113, Japan

and

Kouji Ikeuchi

Engineer, River Division
Civil Engineering Bureau, Tochigi Prefecture
Utsunomiya-shi, Tochigi-ken 320, Japan

SYNOPSIS

The flow in a meandering channel the centerline of which follows a sine-generated curve is analyzed with a perturbation technique. The main emphasis is laid on the transverse shift of the location of the maximum velocity in a section along a unit bend.

The effect of the local radius of curvature is taken into consideration in the present formulation, which results in an improvement of existing theories especially when the width to depth ratio exceeds 10^2. Solutions are obtained up to the second order.

It is revealed that the location of the maximum velocity in a section is strongly dependent on the transverse shape of the bed topography. The typical features of the transverse distribution of the depth-averaged primary flow both in a flat bed and in an equilibrium bed obtained for a movable bed are reproduced by the present theory.

INTRODUCTION

Foreword

A planimetric shape of the centerline of rivers commonly follows consecutively alternating arc-like bends. The flow in bends has been an important subject for both high- and low-stage of water, concerning river embanking and intake of water. The flow in meandering channels is three-dimensional and the characteristics of secondary flows have been reported by many papers. The main emphasis of these previous works, however, is laid on features of a single bend and a fully developed region where the flow does not vary in the longitudinal direction.

In this study the longitudinal variation of the depth-averaged flow is analyzed. The process of convergence and divergence of the flow toward and from the outer bank is considered the most important feature. Consequently, the distribution of the secondary flow is not discussed in this paper.

Terminology

Definitions of the terms used in this paper are given as follows to avoid

confusion.

(i) primary flow: velocity component parallel to the centerline of the channel.

(ii) transverse flow: horizontal velocity component perpendicular to the centerline of the channel. The vertical component does not explicitly appear in this analysis because we are concerned with the depth-averaged velocity field.

(iii) fully developed region: the region where time-averaged hydraulic quantities do not vary in the longitudinal direction.

(iv) depth-averaged velocity: primary and transverse flow components averaged over a local water depth.

(v) equilibrium region: the region where hydraulic quantities show the same value repeatedly at the similar phase of bends. The flow pattern reaches in equilibrium in an idealized meandering channel composed of the similar unit bend which is connected alternately in opposite direction.

Brief Review Of Previous Works

Most of theoretical studies in previous works were devoted to the analysis on the secondary flow in a fully developed region. The fully developed region, however, is a simplification to remove a mathematical difficulty and will be found out in part of a strong bend which has large change in its direction, say, larger than 180 degrees (ex. Kikkawa, Ikeda, Ohkawa and Kawamura(9)). In meandering channels water depth, velocity and flow direction gradually change in the longitudinal direction.

There are several examples which dealt with the transitional characteristics of the flow in a bend. Leschziner and Rodi(12) solved a three-dimensional system of equations for turbulent flow by k-ε model. De Vriend(22) obtained a first order solution of a three-dimensional problem by using a perturbation parameter composed of the ratio of the water depth to the radius of curvature of the centerline. Kalkwijk and de Vriend(8) proposed a depth-averaged form of the Reynolds equations, and the flow behavior was analyzed by a method of characteristics.

Analytical approach to the flow in a bend marked a remarkable advance when Engelund(2) solved the equilibrium features of the flow in a meandering channel the centerline of which was explained by a sine-generated curve. Ikeda et al. (6) further took the effect of superelevation which was neglected in Engelund's analysis into consideration and discussed the development of free meandering of rivers. Hasegawa(3) proposed a shallow water theory over alternating bars and applied double Fourier series to obtain a solution.

Previous analysis by Engelund, Ikeda et al. and Hasegawa et al. implicitly assumed that a radius of curvature at an arbitrary point in a bend is the same as that at the centerline. This assumption involves the error of the order of ε which is equal to the channel width divided by the representative radius of curvature. Therefore, this assumption is considered not suitable for a perturbation analysis using ε as a perturbation parameter. Furthermore, previous solutions are derived under an equilibrium condition. This means that the effect of neither upstream nor downstream boundary conditions was not taken into consideration in existing theories.

Recently studies on the flow in meandering channels have been actively accumulated in various fronts. Hasegawa(4) solved a linearized equation of shallow water flow over alternating bars with the weighted residual method. The obtained result may explain the experimental results on the phase shift of bars against a geometric shape of the channel and on the standing condition for the bar migration. Mori and Kishi(13, 14) studied the effect of interaction between the primary and the transverse flows for a fully developed flow in bends. For a rectangular and an idealized alluvial transverse bed profile, they were able to reproduce the observed results of the main flow distribution in Ishikari River with a two-dimensional scheme of the k-ε model. Demuren(1) studied flow and mass transport characteristics in a rectangular meandering channel with the k-ε model. Tanaka and Ikeda(20) performed both turbulence measurement and

numerical analysis with the k-ε model for a meandering air duct. Tamai and Ikeya(19) developed an analytical three-dimensional approach with the weighted residual method, keeping the major nonlinear term in the momentum equation.

Objectives of the Present Study

The major emphasis is laid on the development of the theory which enables to explain the alternate gradual change of the transverse distribution of the primary velocity in meandering channels. For this purpose it is considered the depth-averaged flow analysis gives sufficiently realistic solutions for river flows, because the width to depth ratio of rivers is pretty large. Furthermore, the effect of the sectional profile of the bed topography on the transverse distribution of the primary flow is explained. A rectangular section and an equlibrium alluvial profile are treated.

An analytical expression is sought because of its clarity to the depth of essence. Being motivated by incompleteness of existing theories, a rigorous formulation of governing equations in a general curvilinear coordinate system for meandering channels is developed at first. Then the linear theory of the perturbation method is extended to the second order in order to bring the perturbation technique to a reasonable level of completion.

This paper is an English version of the Japanese paper written by authors(7) with addition of the review on later studies.

GOVERNING EQUATIONS FOR THE FLOW IN MEANDERING CHANNELS

Coordinate System

According to Langbein and Leopold(10), the centerline of meandering channels in field is expressed by the 'so-called' sine-generated curve.

$$\theta = \theta_0 \sin \frac{2\pi s_c}{L} \tag{1}$$

where θ = angle between the tangent of the centerline of the channel and the direction of the meandering belt, θ_0 = the maximum of θ, L = the meandering length along the centerline, and s_c = the distance along the centerline of the channel. The origin of s_c-coordinate is located at $\theta = 0$ (see Fig.1).

Then n_a coordinate is taken perpendicular to s_c in the same plane on which s_c lies (plane A). The origin of n_a -curve is on the s_c -curve. A curve which connects equal distance points from the s_c -curve on the n_a -curve determines s_a -curve. X -coordinate axis is set at the center of the meandering belt and Y -axis is taken perpendicular to X -axis in the plane A. The origin of (X,Y) coordinate system is determined at the intersection between x -axis and s_c -curve where $\theta = \theta_0$ and $s_c = -L/4$ (see Fig.1).

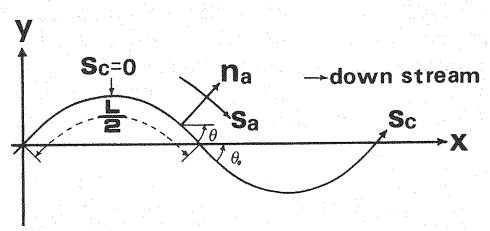

Fig.1 Definition of coordinate system

The relationship between (s_a, n_a) coordinates and (X, Y) coordinates is given as follows:

$$X = \int_{-L/4}^{s_c} \cos\theta \, ds_c + n_a \sin\theta$$

$$Y = \int_{-L/4}^{s_c} (-\sin\theta) \, ds_c + n_a \cos\theta \tag{2}$$

Let $g_{s_a n_a}$ be

$$g_{s_a n_a} = \frac{\partial X}{\partial s_a}\frac{\partial X}{\partial n_a} + \frac{\partial Y}{\partial s_a}\frac{\partial Y}{\partial n_a} \tag{3}$$

The partial differentiation of Eq.3 shows that $g_{s_a n_a}$ is equal to zero, which proves that (s_a, n_a) is coordinates constitute an orthogonal curvilinear coordinate system. Moreover, the radius of curvature at a position (s_a, n_a) is found as in the following equation:

$$r_a = r_c + n_a \tag{4}$$

Geometric Characteristics of the Channel

Several assumptions on the geometry of the meandering channel which are essential to the simplification of governing equations are specifically stated as follows:

i) Depth to width ratio is sufficiently less than unity. The ratio of the depth to the radius of curvature of the channel is sufficiently less than unity, too. Accordingly it is considered that the shear which exerts on the side walls is negligible compared with that on the bottom.

ii) The bed slope of the channel is constant along the centerline of the channel.

iii) The width of the channel is constant.

iv) The centerline of the channel can be explained successfully in terms of a sine-generated curve.

Governing Equations in Terms of Depth-Averaged Velocity

Momentum equations for turbulent flows are often called the Reynolds equations. The three dimensional coordinate system utilized in this paper consists of s_a-, n_a-, z_a-curves. z_a is a coordinate axis taken positive upwards. Based on the assumption 1) aforementioned, it is confirmed that hydrostatic pressure distribution prevails in a shallow and wide flow in meandering channels. Furthermore, smaller terms in the Reynolds stress are neglected due to shallowness and wideness of the flow.

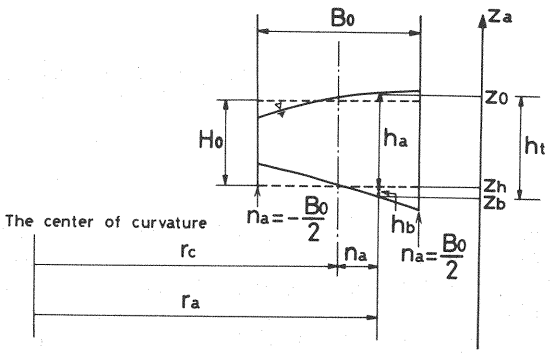

Fig.2 Section of the channel and symbols

Integration of basic equations over the water depth produces a following set of equations. Boundary conditions utilized in the process are as follows: Velocity vanishes on the bottom and the shear vanishes at the water surface.

Equation of continuity is given by

$$\frac{\partial h_t\overline{u_s}}{\partial s_a} + \frac{\partial h_t\overline{u_n}}{\partial n_a} + \frac{h_t\overline{u_n}}{\partial r_a} = 0 \tag{5}$$

where u_s and u_n are velocity components in s_a- and n_a- directions, respectively, h_t is the local water depth and an overbar means the depth-averaged value of attached quantities.

Momentum equation in s_a- direction is given by

$$\frac{\partial h_t\overline{u_s}^2}{\partial s_a} + \frac{\partial h_t\overline{u_s u_n}}{\partial n_a} + 2\frac{h_t\overline{u_s u_n}}{r_a} + gh_t\frac{\partial h_a}{\partial s_a} + gh_t\frac{\partial z_h}{\partial s_a} + \frac{\tau_{s_0}}{\rho} = 0 \tag{6}$$

where $h_a = z_0 - z_h$, $z_0 = z_a$ -coordinate of the water surface, $z_h = z_a$ -coordinate of the transverse mean of the channel bed, ρ = the density of water, and τ_{s_0} = the bed shear stress in s_a -direction.

Momentum equation in n_a -direction is given by

$$\frac{\partial h_t \overline{u_s u_n}}{\partial s_a} + \frac{\partial h_t \overline{u_n}^2}{\partial n_a} + \frac{h_t(\overline{u_n}^2 - \overline{u_s}^2)}{r_a} + g h_t \frac{\partial h_a}{\partial n_a} + \frac{\tau_{n0}}{\rho} = 0 \qquad (7)$$

where τ_{n0} = the bed shear stress in n_a -direction.

Intergration of Eq.5 from $n_a = -B_0/2$ to $n_a = B_0/2$, where B_0 means the width of the channel, gives

$$\int_{-B_0/2}^{B_0/2} h_t \overline{u_s} dn_a = Q = VH_0B_0 \qquad (8)$$

where the condition that $\overline{u_n}$ on both side walls is zero is adopted. In Eq.8 Q is the total discharge, V the representative velocity, H_0 the representative depth. 'Representative' means that the average over the whole region of a single bend.

Boundary conditions are listed as follows:

i) $\overline{u_n} = 0$ at $n_a = \pm B_0/2$ (9)

ii) $\overline{u_s} = \overline{u_{si}}(n_a)$ at $s_c = s_{ci}$ (upstream end) (10)

where $\overline{u_{si}}(n_a)$ denotes a given function of n_a.

iii) $\int_{-B_0/2}^{B_0/2} h_a dn_a = B_0H_0$ at $s_c = s_{ce}$ (downstream end) (11)

Eq.11 means that the sectional average depth is equal to the representative depth at the downstream end.

Correlations of Velocity and Bed Shear Stresses

Assumptions utilized in the following analysis are listed as below.

i) $\overline{u_s u_n} \simeq \overline{u_s} \cdot \overline{u_n}$ (12)

ii) $\overline{u_s}^2 \simeq (\overline{u_s})^2$ (13)

iii) $\overline{u_n}^2 \simeq (\overline{u_n})^2$ (14)

Approximate expressions in Eqs.12 and 13 mean that the primary velocity component is assumed nearly uniform in the vertical direction. Equation 14 shows relatively large error in the fully developed region where $\overline{u_n}$ is zero. The order of the magnitude of the term which involves $\overline{u_n}^2$, however, is comparatively small in basic equations. Consequently, it is supposed that the error due to the approximation in Eq.14 does not produce any significant error in solutions.

Let us consider that the longitudinal component of the bed shear is expressed (6) as,

$$\frac{\tau_{s0}}{\rho} = \frac{1}{2} f (\overline{u_s})^2 \qquad (15)$$

where f = the friction coefficient. It is assumed that the direction of the velocity vector coincides with that of the shear on the bottom. Thus, the following relationship results:

$$\frac{\tau_{n0}}{\tau_{s0}} = \left(\frac{\overline{u_n}}{\overline{u_s}}\right)_{\text{bottom}} \qquad (16)$$

According to Rozovskii(16) and Engelund(2), the next equation has been derived empirically.

$$\left(\frac{\overline{u_n}}{\overline{u_s}}\right)_{\text{bottom}} = (7\sim11)\frac{h_t}{r_a} \qquad (17)$$

Combining Eq.16 with Eqs.15 and 17, we can derive the expression for τ_{n0} as follows:

$$\frac{\tau_{n0}}{\rho} = (3.5\sim5.5) f \cdot (\overline{u_s})^2 \cdot \frac{h_t}{r_a} \qquad (18)$$

Nondimensional Form of the Governing Equations

Nondimentional symbols introduced are as follows:

$u = \overline{u_s}/V$, $v = \overline{u_n}/V$, $s = s_c/R$, $n = n_a/(B_0/2)$, $h = h_a/H_0$, $\eta = h_b/H_0$, $u_i = \overline{u_{si}}/V$, $s_0 = s_{ci}/R$, $s_d = s_{ce}/R$, $\varepsilon = (B_0/2)R$, $F_r = V/\sqrt{gH_0}$, $R = L/2\pi\theta_0$, and $k = 2\pi R/L$, (19)

where $h_b = z_h - z_b$ shows the deviation between a local bed level, z_b and the sectional average z_h. Differentiation with respect to s_a is transformed as in the following equation.

$$\frac{\partial}{\partial s_a} = \frac{r_c}{r_a}\frac{\partial}{\partial s_c} \tag{20}$$

The nondimensional form of Eqs.5 and 8 on the volume discharge is derived as follows:

$$\varepsilon\frac{\partial}{\partial s}\{(h+\eta)u\} + \frac{\partial}{\partial n}\{\frac{r_a}{r_c}(h+\eta)v\} = 0 \tag{21}$$

$$\frac{1}{2}\int_{-1}^{1}(h+\eta)u\,dn = 1 \tag{22}$$

Utilizing Eqs.5, 12, 13, 14, 15 and 18, Eqs.6 and 7 are rewritten and then transformed into the nondimensional forms on use of Eqs.19 and 20.

$$u\frac{\partial u}{\partial s} + \frac{r_a}{r_c}\frac{1}{\varepsilon}v\frac{\partial u}{\partial n} + \frac{R}{r_c}uv = -\frac{1}{Fr^2}\frac{\partial h}{\partial s} + \frac{giR}{V^2} - \frac{c}{2}\frac{r_a}{r_c}\frac{u^2}{h+\eta} \tag{23}$$

$$\frac{r_c}{r_a}\varepsilon u\frac{\partial v}{\partial s} + v\frac{\partial v}{\partial n} - \frac{n_0}{r_a}u^2 = -\frac{1}{Fr^2}\frac{\partial h}{\partial n} + (3.5\sim5.5)f\frac{n_0}{r_a}u^2 \tag{24}$$

where $c = fR/H_0$, $n_0 = B_0/2$, and i = bed slope along the centerline of the channel (in case of a movable bed i denotes the slope of the transverse average level of the bed).

Let us estimate the order of magnitude of the second term in the right hand side of Eq.24. As for the value of ε, Yen(23) reported $\varepsilon = 0.13$ for a representative value of navigable part of the Mississippi and the Missouri rivers. Rozovskii (16) adopted $\varepsilon = 0.56$ in his experiment. In the author's experiment(18) $\varepsilon = 0.30$ was adopted referring the field data reported by Leopold and Wolman(11) and Schumm(17). In Hooke's experiment(5) $\varepsilon = 0.22$. In Yodo river $\varepsilon = 0.27$ is observed at a bend near Hirakata. On the other hand the values of f were reported as follows. In Yen's experiment(23) $0.0043 < f < 0.0054$. In Rozovskii's experiment $f = 0.0054$. In authors' experiment $f = 0.001$ and in Hooke's experiment f ranges from 0.012 to 0.058. The value of $f = 0.014$ is observed in the high water stage in Yodo river. Therefore, it is concluded that the magnitude of f is less than the order of ε^2. The order of n_0/r_a is estimated as below.

$$\frac{n_0}{r_a} = \frac{n_0}{r_c + n_a} = 0\ (\varepsilon) \tag{25}$$

Consequently, we obtain

$$(3.5\sim5.5)\ f\frac{n_0}{r_a} = 0\ (\varepsilon^3) \tag{26}$$

Since we are going to obtain up to the second order solution in ε, we can safely neglect the bed shear stress in the transverse momentum equation. This order estimation was also supported by the experimental data(14).

Boundary conditions are shown in nondimensional form as follows:

i) $v = 0$ at $n = \pm1$ (27)

ii) $u = u_i(n)$ at $s = s_0$ (upstream end) (28)

iii) $\frac{1}{2}\int_{-1}^{1}hdn = 1$ at $s = s_d$ (downstream end) (29)

SOLUTIONS FOR A RECTANGULAR CHANNEL

For the case of a rectangular channel $\eta = 0$ is satisfied in basic equations. Substitution of this condition into Eqs.21, 22, 23, and 24 yields the following set of equations.

$$\varepsilon\frac{\partial}{\partial s}(uh) + \frac{\partial}{\partial n}(\frac{r_a}{r_c}vh) = 0 \tag{30}$$

$$\frac{1}{2}\int_{-1}^{1}uhdn = 1 \tag{31}$$

$$u\frac{\partial u}{\partial s} + \frac{r_a}{r_c}\frac{1}{\varepsilon}v\frac{\partial u}{\partial n} + \frac{R}{r_c}uv = -\frac{1}{F_r^2}\frac{\partial h}{\partial s} + \frac{giR}{V^2} - \frac{c}{2}\frac{r_a}{r_c}\frac{u^2}{h} \tag{32}$$

$$\frac{r_c}{r_a}\varepsilon u\frac{\partial v}{\partial s} + v\frac{\partial v}{\partial n} - \frac{n_0}{r_a}u^2 = -\frac{1}{F_r^2}\frac{\partial h}{\partial n} \tag{33}$$

Perturbed Expression

To solve a set of partial differential equations a perturbation method is introduced in terms of ε. Hydraulic quantities are explained as follows:

$$\begin{aligned} h &= h_0 + \varepsilon h_1 + \varepsilon^2 h_2 + \cdots\cdots\cdots \\ u &= u_0 + \varepsilon u_1 + \varepsilon^2 u_2 + \cdots\cdots\cdots \\ v &= v_0 + \varepsilon v_1 + \varepsilon^2 v_2 + \cdots\cdots\cdots \\ u_i &= fu_{i0}(n) + fu_{i1}(n) + \varepsilon^2 fu_{i2}(n) + \cdots\cdots\cdots \end{aligned} \tag{34}$$

where u_i denotes a transverse distribution of the dimensionless form of the primary flow and the numeral in subscripts shows the order of solutions.

Since ε is given as $\varepsilon = n_0/R$, in the fourth equation of Eq.34 the highest order of n in the function f_{ui} coincides with the order of ε. Accordingly, fu_{i0}, f_{ui1} and f_{ui2} are 0th, linear, and quadratic functions of n, respectively. In order to make the upstream boundary condition be independent of the order of solutions, the following conditions are imposed on the distribution function.

$$\begin{aligned} &\frac{1}{2}\int_{-1}^{1} fu_{i0}(n)dn = 1, \qquad \int_{-1}^{1} fu_{i1}(n)dn = 0 \\ &\int_{-1}^{1} fu_{i2}(n)dn = 0 \end{aligned} \tag{35}$$

Then, Eq.34 is rewritten as in Eq.36 satisfying Eq.35.

$$u_i(n) = u_{i0} + \varepsilon n u_{i1} + \varepsilon^2(n^2 - \frac{1}{3})u_{i2} \tag{36}$$

where u_{i0}, u_{i1} and u_{i2} are constants determined by the upstream boundary condition.

The flow condition is assumed in equilibrium and in quasi-normal flow from macroscopic point of view. Therefore, it is considered that the condition

$$h_0 = 1 \tag{37}$$

is stasfied along the centerline of the channel. Furthermore, the zeroth order solution of the longitudinal velocity, u_0 is a function of s only.

Because we chose $\varepsilon = n_0/R$ as a purturbation parameter, a term of the order of ε^{-1} exists in the momentum equation in s-direction. This is the second term in the left hand side of Eq.32, that is, $v_0\partial u_0/\partial n$. The fundamental solution (zeroth order solution) of u, u_0 , however, is considered a function of s only. Accordingly, we are able to conclude that this term comes to be zero.

$$v_0\frac{\partial u_0}{\partial n} = 0 \tag{38}$$

The solutions in each order of ε are explained in due order and the characteristics of the fundamental solution mentioned above are utilized in the process of solving the equation.

Zeroth Order Solution

Basic equations for the zeroth order solutions are put in order as follows:

$$\frac{1}{2}\int_{-1}^{1} u_0 h_0 dn = 1 \quad \text{(sectional discharge)} \tag{39}$$

$$\frac{\partial}{\partial n}(h_0 v_0) = 0 \quad \text{(eq. of continuity)} \tag{40}$$

$$u_0\frac{\partial u_0}{\partial s} + v_0 n\cos ks\,\frac{\partial u_0}{\partial n} + v_1\frac{\partial u_0}{\partial n} + v_0\frac{\partial u_1}{\partial n} + u_0 v_0 \cos ks$$

$$= -\frac{1}{F_r^2}\frac{\partial h_0}{\partial s} + \frac{giR}{V^2} - \frac{c}{2}\frac{u_0^2}{h_0} \quad (s_a\text{-component of mementum}) \tag{41}$$

$$v_0\frac{\partial v_0}{\partial n} = -\frac{1}{F_r^2}\frac{\partial h_0}{\partial n} \quad (n_a\text{-component of momentum}) \tag{42}$$

Boundary conditions are shown as follows:

$$v_0 = 0 \quad \text{at } n = \pm 1 \tag{43}$$
$$u = u_{i0} \quad \text{at } s = s_0 \tag{44}$$
$$\frac{1}{2}\int_{-1}^{1} h_0\,dn = 1 \quad \text{at } s = s_d \tag{45}$$

Reffering to Eqs.40 and 42, it is derived that both v_0 and h_0 are functions of s only. Consequently, the following solutions results from Eqs.37 and 43.

$$v_0 = 0 \tag{46}$$
$$h_0 = 1 \tag{47}$$

Noting that u_0 is a function of s only, Eqs.39 and 47 lead to the solution for u_0.

$$u_0 = 1 \tag{48}$$

Substitution of Eqs.46, 47, and 48 into Eq.41 yields the following relationship for the condition of the normal flow.

$$\frac{giR}{V^2} = \frac{c}{2} \tag{49}$$

First Order Solution

Basic equations for the first order solutions are shown as follows:

$$\int_{-1}^{1} (u_0 h_1 + u_1 h_0)\,dn = 0 \quad \text{(sectional discharge)} \tag{50}$$

$$\frac{\partial}{\partial s}(u_0 h_0) + \frac{\partial}{\partial n}(h_0 v_0 n\cos ks + h_0 v_1 + h_1 v_0) = 0$$

$$\text{(eq. of continuity)} \tag{51}$$

$$u_0\frac{\partial u_1}{\partial s} + u_1\frac{\partial u_0}{\partial s} + v_0 n\cos ks\frac{\partial u_1}{\partial s} + v_1 n\cos ks\frac{\partial u_0}{\partial s} + v_1\frac{\partial u_1}{\partial s}$$
$$+ \cos ks(u_0 v_1 + u_1 v_0) = -\frac{1}{F_r^2}\frac{\partial h_1}{\partial s} - \frac{c}{2}\frac{u_0^2}{h_0}\left\{n\cos ks + 2\left(\frac{u_1}{u_0}\right)\right.$$
$$\left. - \frac{h_1}{h_0}\right\} \quad (s_a\text{-component of momentum}) \tag{52}$$

$$u_0\frac{\partial v_0}{\partial s} + v_0 n\cos ks\frac{\partial v_0}{\partial n} + v_0\frac{\partial v_1}{\partial n} + v_1\frac{\partial v_0}{\partial n} - u_0^2\cos ks$$
$$= -\frac{1}{F_r^2}\left(n\cos ks\frac{\partial h_0}{\partial n} + \frac{\partial h_1}{\partial n}\right) \quad (n_a\text{-component of momentum}) \tag{53}$$

Boundary conditions are summarized as follows:

$$v_1 = 0 \quad \text{at } n = \pm 1 \tag{54}$$
$$u_1 = nu_{i1} \quad \text{at } s = s_0 \tag{55}$$
$$\frac{1}{2}\int_{-1}^{1} h_1\,dn = 0 \quad \text{at } s = s_d \tag{56}$$

Substituting Eqs.46, 47 and 48 into Eq.51, we obtain the following solution on use of Eq.54.

$$v_1 = 0 \tag{57}$$

Substitution of Eqs.46, 47, 48 and 57 into Eq.53 makes the equation as below.

$$\frac{\partial h_1}{\partial n} = Fr^2 \cos ks \tag{58}$$

Integration of this equation leads to

$$h_1 = nFr^2 \cos ks + F_{h1}(s) \tag{59}$$

where $F_{h1}(s)$ means a function of s only.

Equation 50 is rewritten as in the next equation on use of Eqs.47 and 48.

$$\int_{-1}^{1} (h_1 + u_1) dn = 0 \tag{60}$$

Substitution of Eqs.46, 47, 48 and 57 into Eq.52 leads to Eq.61 as below.

$$\frac{\partial u_1}{\partial s} + cu_1 = -\frac{1}{Fr^2}\frac{\partial h_1}{\partial s} - \frac{c}{2} n \cos ks + \frac{c}{2} h_1 \tag{61}$$

Integrating Eq.61 over the range from n = -1 to n = 1, and using Eqs.59 and 60, we obtain a differential equation to determine $F_{h1}(s)$.

$$(F_r^2 - 1)\frac{\partial F_{h1}(s)}{\partial s} + \frac{3}{2} cFr^2 F_{h1}(s) = 0 \tag{62}$$

Assuming that $F_r^2 \neq 1$ and denoting

$$C_2 = 1.5\, cF_r^2/(F_r^2 - 1), \tag{63}$$

we obtain the expression for $F_{h_1}(s)$ as follows.

$$F_{h_1}(s) = C_1 e^{-C_2 s} \tag{64}$$

where a constant C_1 is determined by a lower boundary condition. Substitution of Eqs.59 and 64 into Eq.56 reveals that $C_1 = 0$. Therefore, nondimensional water depth in the first order is finally obtained as follows.

$$h_1 = nF_r^2 \cos ks \tag{65}$$

The solution for the longitudinal velocity is obtained when we solve Eq.61 with Eq.65 and a boundary condition shown in Eq.55.

$$u_1 = n(A \sin ks + B \cos ks + C_3 e^{-cs}) \tag{66}$$

where

$$\begin{aligned} A &= kc\,(1 + F_r^2)/2(c^2 + k^2) \\ B &= \{0.5c^2(Fr^2 - 1) - k^2\}/(c^2 + k^2) \\ C_3 &= (u_{i1} - A \sin ks_0 - B \cos ks_0) e^{cs_0} \\ c &= fR/H_0 \end{aligned} \tag{67}$$

The solutions up to the first order are summarized as follows:

$$\begin{aligned} h &= h_0 + \varepsilon h_1 = 1 + \varepsilon nFr^2 \cos ks \\ u &= u_0 + \varepsilon u_1 = 1 + \varepsilon n\,(A \sin ks + B \cos ks + C_3 e^{-cs}) \\ v &= v_0 + \varepsilon v_1 = 0 \end{aligned} \tag{68}$$

Second Order Solution

Basic equations in the second order are shown as follows:

$$\int_{-1}^{1} (h_0 u_2 + h_1 u_1 + h_2 u_0) dn = 0 \quad \text{(sectional discharge)} \tag{69}$$

$$\begin{aligned} \frac{\partial}{\partial s}(h_0 u_1 + h_1 u_0) = -\frac{\partial}{\partial n}\{&n \cos ks (h_0 v_1 + h_1 v_0) + h_0 v_2 + h_1 v_1 \\ &+ h_2 v_0\} \quad \text{(eq. of continuity)} \end{aligned} \tag{70}$$

$$u_0\frac{\partial u_2}{\partial s} + u_1\frac{\partial u_1}{\partial s} + u_2\frac{\partial u_0}{\partial s} + v_0\frac{\partial u_3}{\partial n} + v_1\frac{\partial u_2}{\partial n} + v_2\frac{\partial u_1}{\partial s} + v_3\frac{\partial u_0}{\partial n}$$

$$+ \text{ncosks}\ (v_0\frac{\partial u_2}{\partial n} + v_1\frac{\partial u_1}{\partial n} + v_2\frac{\partial u_0}{\partial n}) = -\frac{1}{F_r^2}\frac{2h_2}{\partial s}$$

$$-\frac{c}{2}\frac{u_0^2}{h_0}\left[-2(\frac{u_1}{u_0})(\frac{h_1}{h_0}) + (\frac{u_1}{u_0})^2 + 2(\frac{u_2}{u_0}) + (\frac{h_1}{h_0})^2 - (\frac{h_2}{h_0})\right.$$

$$\left.+ \text{ncosks}\ \{2(\frac{u_1}{u_0}) - (\frac{h_1}{h_0})\}\right] \quad (s_a\text{-component of momentum}) \tag{71}$$

$$u_0\frac{\partial v_1}{\partial s} + u_1\frac{\partial v_0}{\partial s} + v_0\frac{\partial v_2}{\partial n} + v_1\frac{\partial v_1}{\partial n} + v_2\frac{\partial v_0}{\partial n} + \text{ncosks}(v_0\frac{\partial v_1}{\partial n} + v_1\frac{\partial v_0}{\partial n})$$

$$- 2u_1u_0\text{cosks} = -\frac{1}{F_r^2}\frac{\partial}{\partial n}(h_1\text{ncosks} + h_2)$$

$$(n_a\text{-component of momentum}) \tag{72}$$

Boundary conditions are given as follows:

$$v_2 = 0 \qquad \text{at } n = \pm 1 \tag{73}$$

$$u_2 = (n^2 - \frac{1}{3})u_{i2} \qquad \text{at } s = s_0 \tag{74}$$

$$\frac{1}{2}\int_{-1}^{1} h_2 dn = 0 \qquad \text{at } s = s_d \tag{75}$$

Substituting the zeroth and first order solutions (Eqs.46, 47, 48, 57, 65 and 66) into Eq.70, we can determine the expression for v which satisfies the boundary condition of Eq.73 as follows:

$$v_2 = (1 - n^2)(D\text{cosks} + E\text{sinks} + C_4e^{-cs}) \tag{76}$$

where

$$\begin{aligned} D &= kA/2 \\ E &= -k(B + F_r^2)/2 \\ C_4 &= -C_3c/2 \end{aligned} \tag{77}$$

Substituting Eqs.46, 47, 48, 57, 65 and 66 into Eq.72 and solving a differential equation, we obtain the following equation:

$$h_2 = h_{21}(s, n) + h_{22}(s) \tag{78}$$

where

$$h_{21}(s, n) = \frac{F_r^2}{2}(n^2 - \frac{1}{3})\{A\sin 2ks + B_2(\cos 2ks + 1) + 2C_3e^{-cs}\text{cosks}\} \tag{79}$$

In addition $B_2 = B - 0.5$ and $h_{22}(s)$ denotes a function of s only which will be determined in the next step.

Substitution of Eqs.47 and 48 into Eq.69 leads to the following equation:

$$\int_{-1}^{1} u_2 dn = -\int_{-1}^{1}(u_1h_1 + h_2)dn \tag{80}$$

Substitution of Eqs.46, 47, 48, and 57 into Eq.71 makes the next equation.

$$\frac{\partial u_2}{\partial s} + cu_2 = -u_1\frac{\partial u_1}{\partial s} - v_2\frac{\partial u_1}{\partial n} - v_2\text{cosks} - \frac{1}{F_r^2}\frac{\partial h_2}{\partial s} + cu_1h_1 - \frac{c}{2}h_1^2$$

$$-\frac{c}{2}u_1^2 + \frac{c}{2}h_2 - cu_1\text{ncosks} + \frac{c}{2}h_1\text{ncosks} \tag{81}$$

Integrating the both hand sides of Eq.81 from n = -1 to n = 1 and rewriting on use of Eqs.65, 66, 76, 78, 79 and 80, we can derive a differential equation for h_{22} as follows:

$$\frac{\partial h_{22}}{\partial s} + C_2 h_{22} = \frac{F_r^2}{2(F_r^2 - 1)} G_{h22}(s) \tag{82}$$

where $F_r^2 \neq 1$ is assumed and

$$G_{h22}(s) = T_1 \sin^2 ks + T_2 \sin ks \cos ks + T_3 \cos^2 ks + (T_4 \sin ks + T_5 \cos ks) e^{-cs} + T_6 e^{-2cs} \tag{83}$$

The details for coefficients T_1 through T_6 are given in Appendix 1.

Solving Eq.82 with the aid of Eq.75, we can determine the final form of $h_{22}(s)$ as follows:

$$h_{22}(s) = 0.5F_r^2 (A_3 \sin 2ks + B_3 \cos 2ks + D_3 e^{-cs} \sin ks + E_3 e^{-cs} \cos ks + C_5 e^{-2cs} + C_6 + C_7 e^{-cs}) \tag{84}$$

where coefficients A_3, B_3, D_3, E_3, C_5, C_6 and C_7 are shown in Appendix 2.

Then let us determine the function for u_2. Substituting Eqs.65, 66, 76 and 78 into the right hand side of Eq.81. we obtain Eq.85.

$$\frac{\partial u_2}{\partial s} + c u_2 = G_{u2}(s, n) \tag{85}$$

where

$$G_{u2}(s, n) = P_1(n) \sin^2 ks + P_2(n) \sin ks \cos ks + P_3(n) \cos^2 ks + P_4(n) e^{-cs} \sin ks + P_5(n) e^{-cs} \cos ks + P_6(n) e^{-2cs} + P_7(n) \tag{86}$$

and coefficients $P_1(n)$ through $P_7(n)$ are given in Appendix 3.

Solving Eq.85 under the boundary condition of Eq.74, we obtain the following expression for u_2:

$$u_2 = u_{21}(s, n) + C_8(n) e^{-cs} \tag{87}$$

where

$$u_{21}(s, n) = \frac{P_1 + P_3 + 2P_7}{2} + \frac{P_3 - P_1}{2(c^2 + 4k^2)}(c \cos 2ks + 2k \sin 2ks) + \frac{P_2}{2(c^2 + 4k^2)} (c \sin 2ks - 2k \cos 2ks) - \frac{P_4}{k} e^{-cs} \cos ks + \frac{P_5}{k} e^{-cs} \sin ks - \frac{P_6}{c} e^{-2cs} \sin ks + \frac{P_8}{c - C_2} e^{-c_2 s} \tag{88}$$

$$P_8 = \left(\frac{C_2}{2} + \frac{cF_r^2}{4}\right) C_7 \tag{89}$$

$$C_8(n) = \{u_{i2}(n^2 - \frac{1}{3}) - u_{21}(s, n)\} e^{cs_0} \tag{90}$$

Here, the solutions up to the second order are obtained. The solutions are summarized as follows:

$$\begin{aligned} h &= 1 + \varepsilon h_1 + \varepsilon^2 (h_{21} + h_{22}) \\ u &= 1 + \varepsilon u_1 + \varepsilon^2 u_2 \\ v &= \varepsilon^2 v_2 \end{aligned} \tag{91}$$

The details of solution of each order are described in Eqs.65, 66, 76, 79, 84 and 87.

SOLUTIONS FOR THE FLOW OVER AN EQUILIBRIUM MOVABLE BED

An equilibrium bed means that sediment motion into and out of a particular section balances with each other and that bed topography remains constant from temporal point of view. Let us assume that the bed profile is explained as in the following equation (1 and 4).

$$\eta = \left(\frac{r_c + na}{r_c}\right)^{\phi} - 1 \tag{92}$$

where ϕ=constant and Engelund(2) utilized the following expression.

$$\phi = 7 \tan\Phi \tag{93}$$

where Φ = dynamic friction angle.

Odgaard(15) treated the functional form of ϕ. According to his results Eq.93 is suitable for a continuous meandering channel discussed in this paper but is not applicable to a fully developed zone. In the fully developed zone ϕ is a function of the particle Froude number.

The Taylor expansion of Eq.92 gives us a following expression.

$$\eta = \varepsilon n\phi\cos ks + \varepsilon^2 n^2 \frac{\phi(\phi-1)}{2} \cos^2 ks + \cdots\cdots \tag{94}$$

Accordingly, we can determine the expression for perturbed parts as follows:

$$\eta_0 = 0 \tag{95}$$

$$\eta_1 = n\phi\cos ks \tag{96}$$

Equation 95 shows that the zeroth order solutions for an equilibrium bed are the same as those for the case of a rectangular channel. Therefore, the following equation holds.

$$\begin{aligned} h_0 &= 1 \\ u_0 &= 1 \\ v_0 &= 0 \\ giR/V^2 &= c/2 \end{aligned} \tag{97}$$

Rewriting the equations for the first order solutions on use of Eqs.95, 96 and 97, we obtain regously the same equations for the sectional discharge, equation of continuity, and n_a-component of the momentum equation as those in the case of a rectangular channel. However, the term $c\eta_1/2$ is added to the right hand side of Eq.52 for s_a-component of the momentum equation. Applying the same procedure as that in case of a rectangular section, we obtain

$$\begin{aligned} h_1 &= nF_r^2 \cos ks \\ u_1 &= n(A' \sin ks + B' \cos ks + C_3' e^{-cs}) \\ v_1 &= 0 \end{aligned} \tag{98}$$

where

$$\begin{aligned} A' &= kc(1 + F_r^2 + \phi)/2(c^2 + k^2) \\ B' &= \{c^2(F_r^2 + \phi - 1)/2 - k^2\}/(c^2 + k^2) \\ C_3' &= (u_{i_1} - A' \sin ks_0 - B' \cos ks_0) e^{cs_0} \end{aligned} \tag{99}$$

The equation of continuity in the second order of ε is transformed to the next form utilizing Eqs.95, 97 and 98.

$$\frac{\partial v_2}{\partial n} = -\frac{\partial}{\partial s}(u_1 + h_1 + \eta_1) \tag{100}$$

Substituting Eqs.96 and 98 into the right hand side of Eq.100, we obtain the solution for v_2 which satisfies the boundary conditions.

$$v_2 = (1 - n^2)(D'\cos ks + E'\sin ks + C_4'e^{-cs}) \tag{101}$$

where

$$\begin{aligned} D' &= kA'/2 \\ E' &= -k(B' + F_r^2 + \phi)/2 \\ C_4' &= -C_3'c/2 \end{aligned} \tag{102}$$

Substutiting Eqs.97 and 98 into the n-component of the momentum equation, we obtain the following solution.

$$h_{21} = \frac{F_r^2}{2}\left(n^2 - \frac{1}{3}\right)\{A'\sin 2ks + (B' - 0.5)(\cos 2ks + 1) + 2C_3e^{-cs}\cos ks\} \tag{103}$$

where h_{21} explains the deviation from the sectional average water level.

COMPARISON WITH PREVIOUS SOLUTIONS

Previous solutions by Eqngelund(2) and Ikeda et al.(6) are derived for distributions of velocity and water surface level on the assumption that Eq.92 for an equilibrium bed is applicable to a meandering channel. Further assumption applied is the approximation stated below.

$$\frac{\partial}{\partial s_a} = \frac{\partial}{\partial s_c}, \quad (r_c + n_a \doteqdot r_c) \tag{104}$$

The approximation shown in Eq.104 produces an error of the order of ε. In this section the difference between the presently developed solutions and previous ones is explicitly explained in the first order solution because there have been no second order solutions except those developed in this paper.

The first order solution for the nondimensional longitudinal velocity be Ikeda et al.(6) is shown in the following equation.

$$u_1 = n(A_1\sin ks + B_1\cos ks) \tag{105}$$

where coefficients are given by the following equation.

$$\begin{aligned} A_1 &= \frac{kc}{c^2 + k^2}\left(1 + \frac{\phi}{2} + \frac{F_r^2}{2}\right) \\ B_1 &= \frac{1}{c^2 + k^2}\left\{\frac{c^2}{2}(F_r^2 + \phi) - k^2\right\} \end{aligned} \tag{106}$$

The first order solution derived in this paper is described in Eq.98. In an equilibrium range the term which expresses the effect of the boundary condition disappears. Therefore, omitting the term $C_3'e^{-cs}$, Eq.98 is rewritten as:

$$u_1 = n(A'\sin ks + B'\cos ks) \tag{107}$$

$$\begin{aligned} A' &= \frac{kc}{c^2 + k^2}\left\{1 + \frac{\phi}{2} + \frac{1}{2}(F_r^2 - 1)\right\} \\ B' &= \frac{1}{c^2 + k^2}\left\{\frac{c}{2}(F_r^2 + \phi - 1) - k^2\right\} \end{aligned} \tag{108}$$

Let us consider the case of a rectangular channel ($\phi = 0$). The location $s = 0$ corresponds to the apex of the meander. At this location u_1 becomes $u_1 = nB'$, which means that if B' is positive, the velocity along the outer bank is faster and if B' is negative, the opposite situation occurs. Eq.108 shows that B' is always negative for subcritical flows ($F_r<1$). Therefore, the

velocity along the inner bank is the fastest at the apex of the bend, which agrees with experimental results. In previous theories this does not remain true for some combinations of c and F_r.

As the value of ϕ increases, the value of B' turns positive and increases. This means the faster velocity appears along the outer bank. This type of transverse distribution of the primary velocity coincides with those observed in rivers. It is concluded that the faster velocity along the outer bank is caused by the bed profile, that is, larger water depth along the outer bank.

The values of A_1, A', B_1, and B' are plotted against $c = fR/H_0$ for $F_r = 0.5$ and $k = 4/\pi$ (central angle for the change of the direction of a meandering reach is 90 degrees) in Fig.3. In Fig.3 ϕ is set to zero. The variation of A' and B'

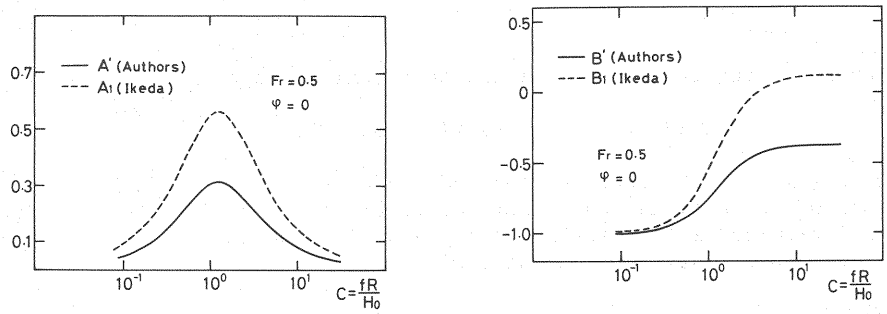

(a) (b)

Fig.3 Improvement of the present theory for a rectangular section

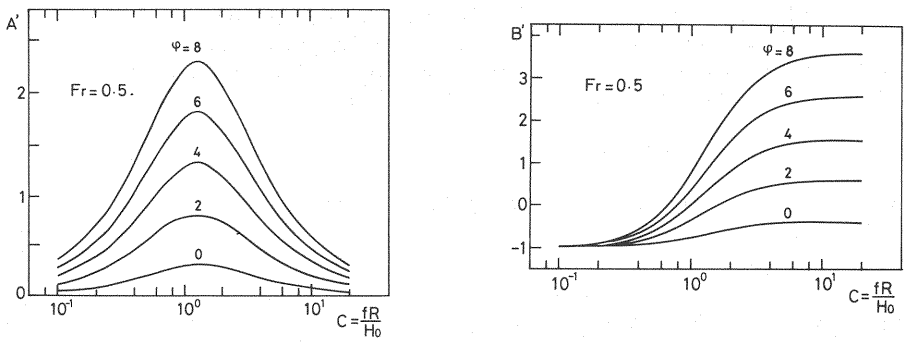

(a) (b)

Fig.4 Coefficients for the depth-averaged primary flow for various bed shapes in the transverse direction

is shown in Fig.4 for various values of ϕ, fixing $F_r = 0.5$ and $k = 4/\pi$. $\phi = 0$ means a rectangular channel and $\phi = 4$ corresponds to Φ = about 30 degrees which was shown in Hooke's experiment (5).

In experimental flumes the value of c is of the order of 10^{-1} or 10^{-2}. Therefore, the error caused by the assumption shown in Eq.104 is not large. However, the order of c in rivers amounting to 10^0 or 10^1, the error caused by Eq. 104 is considerable. The expression of c is rewritten as $c = fR/H_0 = (f/2)(B_0/H_0)\varepsilon^{-1}$. According to field observations during floods, the ratio of surface width to the largest water depth in the section shows the value between 80 and 150 in Tokachi, Omono, Abukuma, Tone, Kuzuryu, Yodo, Hi-i, Yoshino, Niyodo, and Watari Rivers in Japan(21). Furthermore, 70% of data of ε falls into the range from 0.1 to 0.3 in meandering channels (18). These results obtained in field observations infer the order of c stated above.

COMPARISON WITH EXPERIMENTAL RESULTS

Centerline of Experimental Flumes and a Sine-Generated Curve

Most experiments were performed in rectangular channels and their planimetric shape was composed of circular reaches and straight reaches. On the other hand, the theory developed in this paper assumes that the centerline of a flume follows a sine-generated curve. In order to make previous experimental results compatible with the theory, we have to find out a suitable expression for the centerline by a sine-generated curve.

The planimetric shape of Rozovskii's experimental flume which is a single bend and has 180° of central angle in the change of direction is shown in Fig.5 with an approximated sine-generated curve. In the calculation of a sine-generated curve $\theta_0 = \pi/2$ and $L = 2\pi R_0 + 2.5R_0$ are adopted, where R_0 is a radius of curvature along the centerline of a circular channel. Accordance of the shape of a fixed boundary with a computed sine-generated curve is very good except the section 6.5 and 8.0 depicted in the figure.

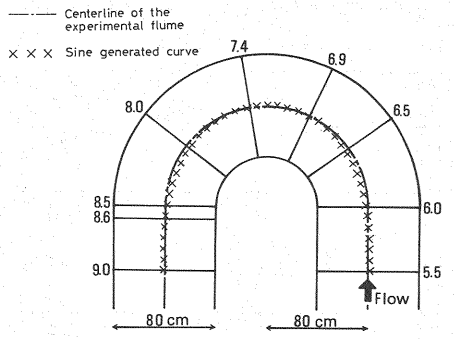

Fig.5 Planimetric shape of a flume used by Rozovskii

Fig.6 shows comparison between Yen's experimental flume and a sine-generated curve approximated. $\theta_0 = \pi/4$ and L is set equal to the distance of a unit bend along the centerline of the experimental flume. It is seen that the centerline of the flume composed of a circle and a straight line can be well approximated by a sine-generated curve.

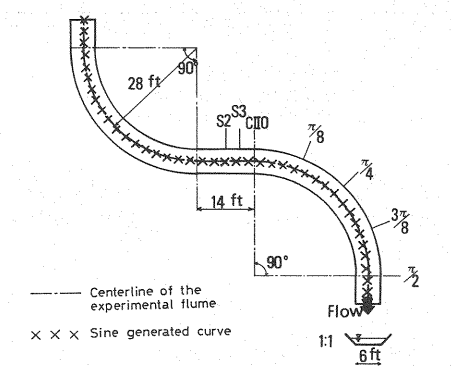

Fig.6 Planimetric shape of a flume used by Yen

The authors performed the experiment in a flume which had ten consecutive bends in the central part and the bed slope of which was constant along the centerline. Accordance between the actual centerline of the flume and a sine-generated curve is good as shown in Fig.7.

Comparison of Rozovskii's Results with Theoretical Results

Experimental conditions utilized in Rozovskii's Experiment No.1 were $\theta_b = 180°$ (the central angle of the change), $R_0 = 0.8$m, $B_0 = 0.8$m, $F_r = 0.34$, $H_0 = 6$ cm (at the entrance to a bend), $V = 0.26$m/s (at the entrance to a bend), Chezy's coefficient = 60 (in m, s unit), and the sectional shape rectangular. Experimental results of the depth-averaged primary velocity are shown in Fig.8 with the theoretical results of the first order solution (Eq.68) and the second order solution (Eq.91). As for the upper boundary condition, $u_{i1} = -0.0142$ and $u_{i2} = -0.575$ are determined by the least square method applied to experimental results.

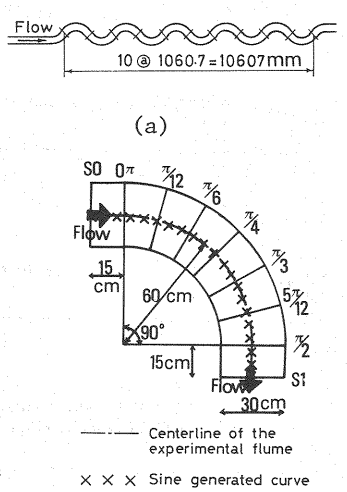

Fig.7 Planimetric shape of a flume used by authors

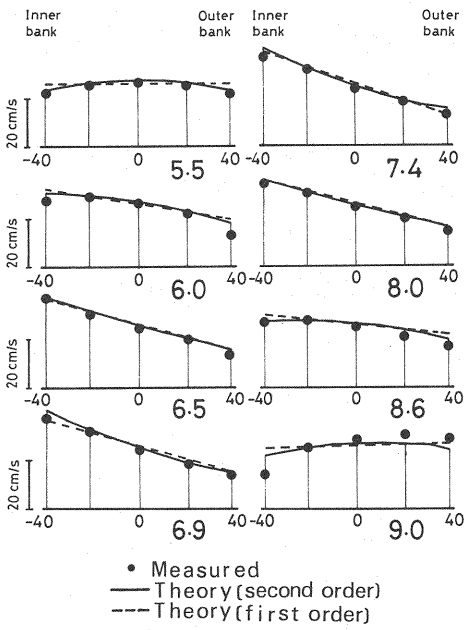

Fig.8 Comparison of Rozovskii's experimental result with the theory (primary velocity)

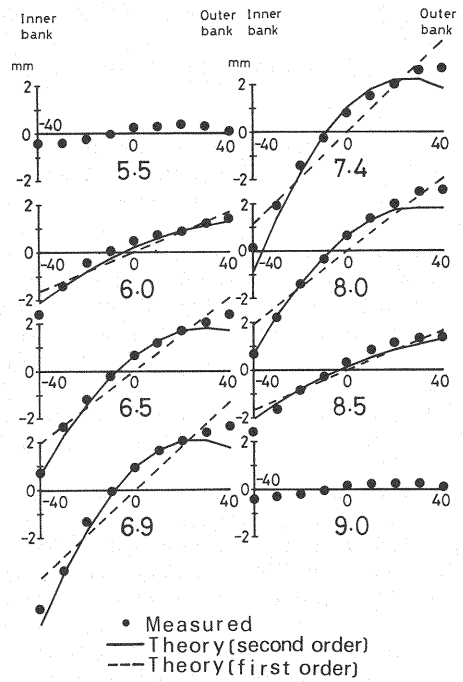

Fig.9 Comparison of Rozovskii's experimental result with the theory (water surface level)

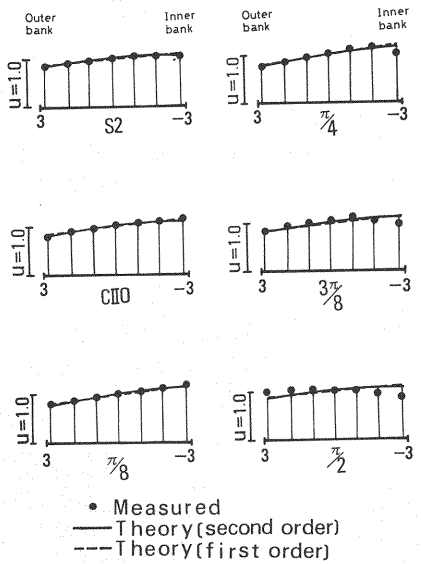

Fig.10 Comparison of Yen's experimental result with the theory (primary velocity, dimensionless expression, u=1 shows sectional average)

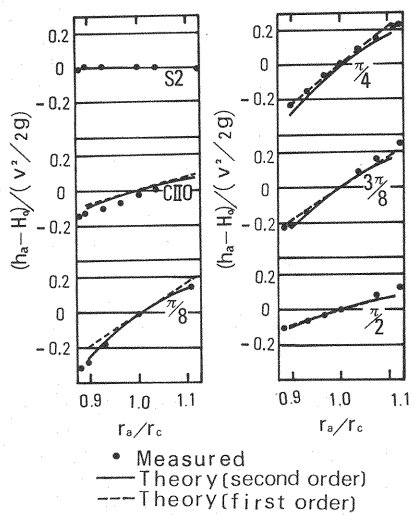

Fig.11 Comparison of Yen's experimental result with the theory (water surface level)

The agreement between observed and theoretical results is good and there is little difference between the first and second order solutions.

Transverse distribution of water surface level is shown in Fig.9. The origin of the vertical coordinate is settled at the mean surface level of each section. Therefore, $h_2 = h_{21}$ in the second order solution(see Eq.78). It is seen that the first order solution is not able to explain the experimental results but the second order solution agrees very well with the experimental results except in the region near the outer bank.

Rozovskii's experiment was performed in flume which had large ratio of the width to radius of curvature. Good accordance with experimental results inferred that the theory was applicable even to the case that $\varepsilon = 0.564$.

Comparison of Yen's Results with Theoretical Results

Quantities utilized in Yen's Run 3 were as follows: $\theta_b = 90°$, $r_c = 8.53$m, $B_0 = 1.83$m (the bottom width), $F_r = 0.58$, $H_0 = 0.156$m (sectional average water depth at the mid-point of the tangent reach between two circular parts), $V = 0.691$m/s (mid-point of the tangent reach), $i_s = 0.00072$ (surface gradient), trapezoidal section, gradient of the side walls 1:1 and $f = 2gH_0i_s/V^2 = 0.0046$.

In Fig.10 observed results and theoretical estimations of the depth-averaged primary velocity are shown. $u_{i1} = -0.955$ and $u_{i2} = -6.194$ are given to explain the observed velocity distribution at the upstream boundary through the least-square-method. Agreement between the observed results and the theoretical results is good except the region near the outer bank in the lower reach and the far downstream section. Discrepancy between the first and the second order solutions is little.

Transverse distribution of water surface level is shown in Fig.11. It is seen that the second order solutions give sufficiently close estimates to experimental results.

Although Yen's experiment was performed in a trapezoidal channel, depth-width ratio was sufficiently small compared with unity. Therefore, the theoretical estimates for a rectangular channel are in good agreement except in the region near the sloping side walls.

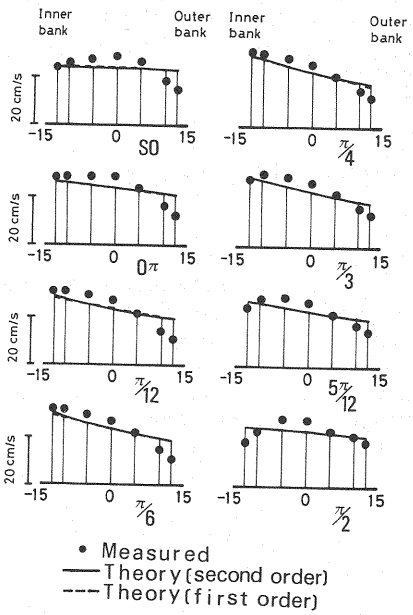

Fig.12 Comparison of author's experimental result with the theory (primary velocity)

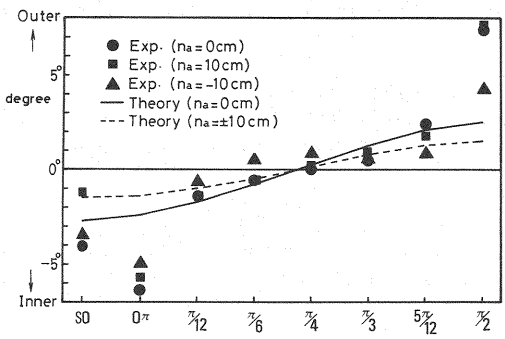

Fig.13 Comparison of author's experimental result with the theory

Comparison of Author's Experimental Results with Theoretical Results

Hydraulic conditions of our experiment were as follows: $\theta_b = 90°$, $r_c = 0.60$m, $B_0 = 0.30$m, $F_r = 0.42$, $H_0 = 2.93$cm (average depth over a bend), $V = 0.223$m/s (=discharge/($H_0 \cdot B_0$)), $i = 1/1000$ (along the centerline of the channel), and $f = 0.0115$.

The depth-averaged primary velocity observed and theoretically estimated is shown in Fig.12. Theoretical results are obtained under the condition of equilibrium range, which means the terms proportional to $e^{-\zeta s}$ are neglected. Theoretical results near the outer bank are larger than those measured. Measured velocity around the center of the channel tends to be larger than that estimated by the theory. In this experiment width-depth ratio was ten, which is relatively small in comparison with actual rivers. Although the agreement between the experiment and the theory is fairly good, transverse distribution of the primary velocity seems to be affected by side walls in the case of a relatively narrow channel.

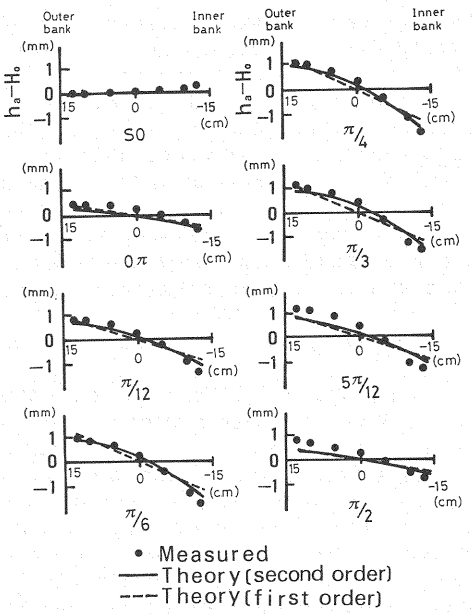

Fig.14 Comparison of author's experimental result with the theory (water sirface level)

Direction derived from depth-averaged velocity vector is shown in Fig.13 with the computed value by arctan $\{\varepsilon^2 v_2/(u_0 + \varepsilon u_1 + \varepsilon^2 u_2)\}$. At the locations of 0π and $\pi/2$ which correspond the entrance and exit of a bend, respectively, the observed values jump to certain large values. Since the radius of curvature varies discontinuously at these points in the experimental flume, the observed values much deviate at these points. However, the theoretical results agrees fairly well with the observed results except at around these two locations.

Transverse distribution of water surface level is shown in Fig.14. The origin of the vertical coordinate is set to the mean surface level of each section. The second order solutions can reproduce the measured results satisfactorily.

Summary of the Comparison Between the Experimental Results and the Theoretical Results

Theoretical results obtained in this paper agree well with experimental results of Rozovskii, Yen, and authors in the transverse distributions of the depth-averaged primary velocity, the direction of the velocity vector, and the water surface level. In the theory it is pointed out that the maximum primary velocity appears along the inner bank in all sections of a bend in the case of a rectangular channel. This is proved in all experimental results referred in this paper. As for the estimation for the water surface level, the second order solutions are neeced for reasonable agreement with experimental results. However, the second order solutions did not show much superiority to the first order solutions for the transverse distribution of the depth-averaged primary velocity.

CONCLUSIONS

Concluding remarks derived in this paper are summarized as in the following items.

1) Up to the second order solutions on the depth-averaged flow field and the water surface level are obtained for meandering channels by perturbation theory. The perturbation parameter ε is defined by ε = (half width of the channel)/(minimum radius of curvature). The solution is rigorously developed for an arbitrary position in a meandering channel, which improves previous theories in which the solution is obtained only along the centerline of the channel. The effect of this improvement becomes explicit when the width to depth ratio exceeds one hundred as encountered in big rivers.
2) According to the theoretical result, the transverse distribution of the depth-averaged primary flow is strongly dependent on bed topography. For sub-critical flows, the maximum primary velocity appears along the inner bank all through a bend in case of a rectangular section and it appears near the outer bank for an equilibrium shape for a movable bed in which deep scour hole exists near the outer bank. The theoretical estimation for the transverse distribution of the depth-averaged primary velocity agrees with measured results in experimental flumes and rivers.
3) Theoretical results are compared with experimental results obtained by Rozovskii, Yen, and authors. Accordance between the theoretical results and measured results is good in the water surface level and the depth-averaged primary velocity. However, the reproducibility of the primary velocity distribution near the exit of a unit bend is less satisfactory.
4) Deviation of the depth-averaged velocity vector from the direction of the centerline coincides with the observed results except for the connecting point between a straight reach and a circular part where the radius of curvature is discontinuous in testing flumes.
5) As for the transverse variation of the water surface, the second order solution provides much better agreement with experimental results. On the contrary, the second order solution gives practically the same result as the first order solution for the depth-averaged primary velocity.

REFERENCES

1. Demuren, A.O.: Three dimensional numerical computation of flow and pollutant dispersion in meandering channels, Proc. XXth Congress, IAHR, Vol.III, pp.29-36, 1983.
2. Engelund, F.: Flow and bed topography in channel bends, Proc. ASCE, J. Hyd. Div., Vol.100, HY11, pp.1631-1647, 1974.
3. Hasegawa, K.: Flow on alternating bars in a straight and a meandering channels, Proc. 36th Annual Meeting, Japan Soc. Civil Engineers, Sec.11, pp.521-522, 1981 (in Japanese).
4. Hasegawa, K.: A study on flows and bed topographies in meandering channels, Proc. JSCE, No.338, pp.105-114, 1983 (in Japanese).
5. Hooke, R. L.: Shear-stress and sediment distribution in a meander bend, UNGI-report 30, Univ. of Uppsala, 58p., 1974.
6. Ikeda, S., M. Hino and H. Kikkawa: Theoretical study on the free meandering of rivers, Proc. JSCE, No.255, pp.63-73, 1976 (in Japanese).
7. Ikeuchi, K. and N. Tamai: Evolution of the depth-averaged flow field in meandering channels, Proc. JSCE, No.334, pp.89-101, 1983 (in Japanese).
8. Kalkwijk, J.P. Th. and H.J. de Vriend: Computation of the flow in shallow river bends, J. Hyd. Research, IAHR, Vol.18, No.4, pp.327-342, 1980.
9. Kikkawa, H., S. Ikeda, H. Ohkawa and Y. Kawamura: Secondary flow in a bend of turbulent stream, Proc. JSCE, No.219, pp.107-114, 1973.
10. Langbein, W.B. and L.B. Leopold: River meanders-theory of minimum variance, U.S.G.S. Prof. Paper 422-H, 15p., 1966.
11. Leopold, L.B. and M.G. Wolman: River meanders, Bullentin of the Geological Soc. America, Vol.71, pp.769-793, 1960.
12. Leschziner, M.A. and W. Rodi: Calculation of strongly curved open channel flow, Proc. ASCE, J. Hyd. Div., Vol.105, HY10, pp.1297-1314, 1979.
13. Mori, A., T. Kishi and M. Yoshioka: A study on the secondary flow in open channel bend, Proc. 27th. Japanese Conf. on Hydraulics, JSCE, pp.79-84, 1983 (in Japanese).

14. Mori, A. and T. Kishi: A study on the secondary flow in open channel bend with transverse sloping bed, Proc. 28th. Japanese Conf. on Hydraulics, JSCE, pp.751-755 (in Japanese).
15. Odgaard, A. J.: Transverse bed slope in alluvial channel bends, Proc. ASCE, J. Hyd. Div., Vol.107, HY12, pp.1677-1694, 1981.
16. Rozovskii, I.L.: Flow of Water in Bends of Open Channels, Israel program for scientific translations, 233p., 1961.
17. Schumm, S.A.: The shape of alluvial channels in relation to sediment type, U.S.G.S. Prof. Paper 352-B. 30p., 1960.
18. Tamai, N., K. Ikeuchi, A. Yamazaki and Ali Mohamed: Experimental analysis on the open channel flow in rectangular continuous bends, J. Hydroscience and Hydraulic Eng., JSCE, Vol.1, No.2, pp.17-31, 1983.
19. Tamai, N. and T. Ikeya: An analytical three-dimensional approach to the flow in rectangular meandering channels, Proc. 4th Congress, Asian and Pacific Regional Div., IAHR, Vol.1, pp.831-845, 1984.
20. Tanaka, M. and S. Ikeda: Three-dimensional numerical analysis of turbulent flow in a sinuous air duct, Proc.39th Annual Meeting, JSCE, Div, pp.471-472, 1984 (in Japanese).
21. Task Committee of the Ministry of Construction: Data Book of Roughness Coefficients in Japanese Rivers, 535p., 1974 (in Japanese).
22. de Vrient, H. J.: A mathematical model of steady flow in curved shallow channels, J. Hyd. Res., Vol.15, No.1, pp.37-54, 1977.
23. Yen, B. C.: Characteristics of subcritical flow in a meandering channel. Institute of Hydraulic Research, Univ. of Iowa, 77p., 1965.

APPENDIX 1 - Coefficients in Eq.83

$$T_1 = (-2ABk + 2F_r^2kA + 4AE + cA^2)/3$$
$$T_2 = (2A^2k - 2B^2k + 4F_r^2Bk + 4AD + 4BE + 4E - 2cAF_r^2 + 2ABc - 2cAF_r^2 + 2Ac)/3$$
$$T_3 = (2ABk - 2F_r^2AK + 4DB + 4D - 4cBF_r^2 + cB^2 + cF_r^4 + 2cB - cF_r^2)/3$$
$$T_4 = (2BkC_3 + 2F_r^2kC_3 + 4EC_3 + 4AC_4)/3$$
$$T_5 = (2AkC_3 + 2F_r^2cC_3 + 4DC_3 + 4BC_4 + 4C_4 - 4cC_3F_r^2 + 2cC_3)/3$$
$$T_6 = -cC_3^2$$

APPENDIX 2 - Coefficients in Eq.84

$$A_3 = \frac{2k(T_3 - T_1) + C_2T_2}{2(C_2^2 + 4k^2)(F_r^2 - 1)} \qquad B_3 = \frac{C_2(T_3 - T_1) - 2kT_2}{2(C_2^2 + 4k^2)(F_r^2 - 1)}$$

$$D_3 = \frac{(C_2 - c)T_4 + kT_5}{\{(C_2 - c)^2 + k^2\}(F_r^2 - 1)} \qquad E_3 = \frac{-kT_4 + (C_2 - c)T_5}{\{(C_2 - c\}^2 + k^2\}(F_r^2 - 1)}$$

$$C_5 = \frac{T_6}{(C_2 - 2c)(F_r^2 - 1)} \qquad C_6 = \frac{T_1 + T_3}{2C_2(F_r^2 - 1)}$$

$$C_7 = -e^{c2sd}(A_3\sin 2ks_d + B_3\cos 2ks_d + D_3e^{-csd}\sin ks_d + E_3e^{-csd}\cos ks_d + C_5e^{-2csd} + C_6)$$

APPENDIX 3 - Coefficients in Eq.86

$$P_1(n) = n^2(ABk + AE + Ak - cA^2/2) - AE - Ak/3 + A_3k - cF_r^2B_3/4$$
$$P_2(n) = n^2(B^2k - A^2k + AD + BE + E + 2kB_2 + 3cAF_r^2/2 - cAB - cA) - AD-BE-E-2kB_2/3 + 2kB_3 - cAF_r^2/6 + cA_3F_r^2/2$$
$$p_3(n) = n^2(-ABk + BD + D - kA + cBF_r^2 - cB^2/2 - cF_r^4/2 + cF_r^2B_2/2 - cB + cF_r^2/2) - BD - D + kA/3 - kA_3 - cB_2F_r^2/6 + cF_r^2B_3/4$$

$$P_4(n) = n^2(BkC_3 + AcC_3 + EC_3 + AC_4 + C_3k - cAC_3) - EC_3 - AC_4 - C_3k/3 + D_3k/2 + E_3c/2 + cF_r^2E_3/4$$
$$P_5(n) = n^2(C_3cB - C_3Ak + DC_3 + BC_4 + C_4 + 3C_3cF_r^2/2 - C_3cB) - DC_3 - BC_4 - C_4 - C_3c/3 + D_3c/2 - E_3k/2 - cC_3F_r^2/6 + cD_3F_r^2/4$$
$$P_6 = -C_3C_4 + cC_5 + cF_r^2C_5/4$$
$$P_7 = cC_6F_r^2/4$$

APPENDIX - NOTATION

The following symbols are used in this paper:

B_0 = width of a meandering channel;

c = fR/H_0;

F_r = $V/\sqrt{gH_0}$;

f = friction coefficient;

f_{ui_0}, f_{ui_1}, f_{ui_2} = zeroth, first, and second order functions to explain nondimensional transverse distribution of the primary flow at the upstream boundary;

$G_{h_{22}}$ = function shown by Eq.83 concerning the second order solution for the water depth;

G_{u_2} = function shown by Eq.86 concerning the second order solution for the primary velocity;

g = gravitational acceleration;

$g_{s_an_a}$ = Jacobian of coordinate transformation between (X, Y) and (s_a, n_a) systems;

H_0 = average depth over a single bend;

h_t = local water depth;

h_a = water depth measured from the sectional average level of the bottom;

h = h_a/H_0;

h_0, h_1, h_2 = zeroth, first, and second order solutions for h, respectively;

h_{21}, h_{22} = two parts of h_2 which are explained in Eqs.79 and 84;

i = bed slope along the centerline of a meandering channel (in case of a movable bed i denotes the slope of the transversely averaged level of the bed);

k = $2\pi R/L$;

L = meandering length along the centerline;

n_0 = $B_0/2$;

n_a = coordinate taken perpendicular to s_c in the same plane on which s_c lies;

n = $n_a/(B_0/2)$;

Q = total discharge;

R = minimum radius of curvature of a meandering channel ($= L/2\pi\theta_0$);

r_a = radius of curvature to an arbitrary point in a section;

r_c = radius of curvature of the centerline of a meandering channel;

s_c = distance along the centerline of a meandering channel;

s_a = coordinate parallel to s_c and perpendicular to n_a;

s_{ci}, s_{ce} = values of s_c at upstream and downstream boundaries, respectively;

s, s_0 , s_d = s_c/R, s_{ci}/R, and s_{ce}/R, respectively;

u_s, u_n, u_z = s_a, n_a, and z components of local velocity, respectively;

$\overline{u_s}$, $\overline{u_n}$ = depth-averaged values of u_s and u_n, respectively;

$\overline{u_{si}}$ = transverse distribution function of $\overline{u_s}$ at the upstream boundary;

u = $\overline{u_s}/V$;

u_0, u_1, u_2 = zeroth, first, and second order solutions for u, respectively;

u_i = $\overline{u_{si}}/V$;

u_{21} = equilibrium component of u_2 which is free from the upstream boundary condition;

V = representative velocity for a unit bend;

v = $\overline{u_n}/V$;

v_0, v_1, v_2 = zeroth, first, and second order solutions for v, respectively;

X, Y = Cartesian coordinate in which X-axis coincides with the centerline of the meandering belt;

z_a = vertical coordinate taken positive upward;

z_0, z_h, z_b = values of z_a-coordinate for the water surface, the transverse mean level of the bed, and the local bed level, respectively;

A, B, C_3 = coefficients shown in Eq.67;

A', B', C_3' = coefficients shown in Eq.99;

B_2 = $B - 0.5$;

C_2 = exponent which explains the effect of the boundary condition Eq.63 ;

D, E, C_4 = coefficients shown in Eq.77;

D', E', C'_4 = coefficients shown in Eq.102;

$T_1 \sim T_6$ = coefficients shown in Appendix 1;

A_3, B_3, D_3, E_3, $C_5 \sim C_7$ = coefficients shown in Appendix 2;

$P_1(n) \sim P_7(n)$ = coefficients shown in Appendix 3;

P_8 = coefficients shown in Eq.89;

η = h_b/H_0;

ε = perturbation parameter (= $(B_0/2)$ /R);

θ = angle between the tangent of the centerline of a meandering channel and the direction of the meandering belt;

θ_0 = maximum value of θ;

ϕ = exponent in Eq.92;

Φ = dynamic friction angle; and

τ_{s_0}, τ_{n_0} = bed shear stress in s_a and n_a directions, respectively.